



This discussion paper is/has been under review for the journal Hydrology and Earth System Sciences (HESS). Please refer to the corresponding final paper in HESS if available.

The Budyko framework beyond stationarity

P. Greve^{1,2,*}, L. Gudmundsson¹, B. Orlowsky¹, and S. I. Seneviratne¹

¹Institute for Atmospheric and Climate Science, ETH Zurich, Zurich, Switzerland

²Center for Climate Systems Modeling (C2SM), ETH Zurich, Zurich, Switzerland

* *Invited contribution by P. Greve, recipient of the EGU Outstanding Student Poster Award 2014.*

Received: 08 June 2015 – Accepted: 17 June 2015 – Published: 16 July 2015

Correspondence to: P. Greve (peter.greve@env.ethz.ch)

Published by Copernicus Publications on behalf of the European Geosciences Union.

Title Page

Abstract

Introduction

Conclusions

References

Tables

Figures



Back

Close

Full Screen / Esc

Printer-friendly Version

Interactive Discussion



Abstract

Water availability is of major importance for a wide range of socio-economic sectors. Over land, the partitioning of precipitation (P) into evapotranspiration (E) and runoff (Q) is the key process to assess hydrological conditions. For climatological averages, the Budyko framework provides a simple first order relationship to estimate the evaporative index E/P as a function of the aridity index (E_p/P , with E_p denoting potential evaporation). However, a major downside of the Budyko framework is its limitation to steady state conditions, being a result of the assumption of a closed land water balance. Nonstationary processes coming into play at other than mean annual catchment scales are thus not represented. Here we propose an analytically derived new formulation of the Budyko curve including an additional parameter being implicitly related to the nonlinear storage term of the land water balance. The new framework is comprehensively analysed, showing that the additional parameter leads to an upward rotation of the original supply limit and therefore implicitly represents the amount of additional water available for evaporation. The obtained model is further validated using standard datasets of P , E and E_p . It is shown that the model is capable to represent first-order seasonal dynamics within the hydroclimatological system.

1 Introduction

The Budyko framework serves as a tool to predict mean annual water availability as a function of aridity. It is widely-used and well-established within the hydrological community, both due to its simplicity and long history, combining experience from over a century of hydrological research. Since Budyko (1956, 1974) derived a formulation of the curve based on findings of Schreiber (1904) and Ol'Dekop (1911), several other formulations have been postulated, which however are numerically surprisingly similar (Schreiber, 1904; Ol'Dekop, 1911; Turc, 1955; Mezentsev, 1955; Pike, 1964; Fu, 1981; Choudhury, 1999; Zhang et al., 2001, 2004; Porporato et al., 2004; Yang et al., 2008;

HESSD

12, 6799–6830, 2015

Nonstationary Budyko framework

P. Greve et al.

Title Page

Abstract

Introduction

Conclusions

References

Tables

Figures

⏪

⏩

◀

▶

Back

Close

Full Screen / Esc

Printer-friendly Version

Interactive Discussion



Nonstationary
Budyko framework

P. Greve et al.

Title Page

Abstract

Introduction

Conclusions

References

Tables

Figures

I◀

▶I

◀

▶

Back

Close

Full Screen / Esc

Printer-friendly Version

Interactive Discussion



Donohue et al., 2012; Wang and Tang, 2014; Zhou et al., 2015b). Many of these formulations are empirically derived and only few are analytically determined from simple phenomenological assumptions (Fu, 1981; Milly, 1994; Porporato et al., 2004; Zhang et al., 2004; Yang et al., 2007). Nonetheless, derived functional forms in all formulations are deterministic and assessments on controls determining the observed systematic scatter around the mean Budyko curve have been subject to numerous studies. A variety of catchment and climate characteristics, such as e.g. vegetation (Zhang et al., 2001; Donohue et al., 2007; Williams et al., 2012; Li et al., 2013; Zhou et al., 2015a), seasonality characteristics (Milly, 1994; Potter et al., 2005; Gentine et al., 2012; Chen et al., 2013; Berghuijs et al., 2014), soil properties (Porporato et al., 2004; Shao et al., 2012; Donohue et al., 2012), and topographic controls (Shao et al., 2012; Xu et al., 2013) have been proposed to exert a certain influence on the scatter within the Budyko space. Also complex hybrids of various controls (Milly, 1994; Gentine et al., 2012; Donohue et al., 2012; Xu et al., 2013) have been considered, but until present, no conclusive statement on controls were made.

In this study we make use of the formulation derived by Fu (1981) and Zhang et al. (2004). They derive the following functional form between E/P and $\Phi = E_p/P$ analytically from simple physical assumptions:

$$\frac{E}{P} = 1 + \Phi - (1 + (\Phi)^\omega)^{\frac{1}{\omega}}, \quad (1)$$

where ω is a free model parameter ($\omega = 2.6$ results in the original Budyko curve). The obtained curve is subject to two physical constraints constituting both the water demand and supply limit. The water demand limit represents E being limited by E_p , whereas the water supply limit determines E to be limited by P (see Fig. 1). Hence, the supply limit requires steady-state conditions. The storage term (dS/dt) in the land water balance equation

$$\frac{dS}{dt} = P - E - Q \quad (2)$$

Nonstationary Budyko framework

P. Greve et al.

Title Page

Abstract

Introduction

Conclusions

References

Tables

Figures

◀

▶

◀

▶

Back

Close

Full Screen / Esc

Printer-friendly Version

Interactive Discussion



is consequently neglected, a generally valid approach at mean annual catchment scales. Although we note, that year to year changes in soil moisture may happen, e.g. under transient climate change (Wang, 2005; Orlowsky and Seneviratne, 2013). However, the assumption of steady-state conditions does not permit the usage of the Budyko framework at monthly to seasonal time scales and constitutes a major limitation of the framework. Only few assessments addressed this limitation. Potter and Zhang (2007) derived a formulation based on previous work by Milly (1993) in order to model interstorm E . In a comprehensive top-down approach, Zhang et al. (2008) developed a water balance model for subannual to mean annual time scale. They suggested that model complexity has to increase at intrannual time scales to account for soil-moisture dynamics, and they extended the Budyko model accordingly by introducing four additional parameters. Chen et al. (2013) extended the Budyko model to seasonal time scales by introducing a seasonal aridity index that accounts for storage changes. Although these approaches provide interesting insights on the Budyko hypothesis at subannual time scales, they are still derived empirically. Nevertheless, all approaches agree on the necessity to include storage changes, but so far a robust, theoretical incorporation into the Budyko framework is missing.

In this work, we aim to analytically derive a new Budyko formulation for dynamic conditions at e.g. subannual time scales. Our approach is based on simple phenomenological assumptions in which the storage term is implicitly considered. This is achieved by reformulating the set of differential equations given in Fu (1981) and Zhang et al. (2004) such that the water supply limit is no rigid physical constraint.

2 Deriving a new formulation

2.1 Preliminary assumptions

On the basis of Fu (1981) and Zhang et al. (2004), we postulate that for a given potential evaporation, the rate of change in evapotranspiration as a function of

precipitation ($\partial E/\partial P$) increases with residual potential evaporation ($E_p - E$) and decreases with precipitation. Similar assumptions are made regarding the rate of change in evapotranspiration as a function of potential evaporation ($\partial E/\partial E_p$) by considering residual precipitation ($P - E$). Hence, both ratios can be written as

$$\frac{\partial E}{\partial P} = f(x) \quad (3a)$$

$$\frac{\partial E}{\partial E_p} = g(y) \quad (3b)$$

with

$$x = \frac{E_p - E}{P} \quad (4a)$$

$$y = \frac{P - E}{E_p} \quad (4b)$$

Considering E_p being a natural constraint of E , it follows

$$\left. \frac{\partial E}{\partial P} \right|_{x=0} = 0 \quad (5)$$

The original approach of Fu (1981) further assumes that P is a natural constraint of E , giving the following boundary condition

$$\left. \frac{\partial E}{\partial E_p} \right|_{y=0} = 0. \quad (6)$$

This assumption requires steady-state conditions and is consequently valid at mean annual catchment scales (such that $P - E \geq 0$) only. However, due to storage changes, on shorter time scales and smaller spatial scales $E \geq P$ (respectively, $y \leq 0$) is possible.

Nonstationary Budyko framework

P. Greve et al.

Title Page

Abstract

Introduction

Conclusions

References

Tables

Figures

⏪

⏩

◀

▶

Back

Close

Full Screen / Esc

Printer-friendly Version

Interactive Discussion



In this case E_p remains the only constraint of E . The minimum value y_{\min} of y thus lies within the interval between -1 and 0 and depends on the additional amount of water being available for evaporation (and thus implicitly refers to the storage term in Eq. 2). For convenience we define $y_0 = -y_{\min}$ (and thus $y_0 \in [0, 1]$). The boundary condition (6) is then redefined as

$$\left. \frac{\partial E}{\partial E_p} \right|_{-y_0} = 0. \quad (7)$$

2.2 Solution

Solving the system of the differential equations (3a,b) using boundary condition (5) and the new condition (7) yields the following solution (details are provided in Appendix A):

$$E = E_p + P - \left((1 - y_0)^{\kappa-1} E_p^\kappa + P^\kappa \right)^{\frac{1}{\kappa}} \quad (8)$$

with κ being a free model parameters. It follows

$$\frac{E}{P} = F(\Phi, \kappa, y_0) = 1 + \Phi - \left(1 + (1 - y_0)^{\kappa-1} (\Phi)^\kappa \right)^{\frac{1}{\kappa}}. \quad (9)$$

Similar to the traditional Budyko approach a free model parameter (named κ to avoid confusion with the traditional ω) is obtained. The parameter y_0 is directly related to the new boundary condition. Hence, in contrast to κ , which is a mathematical constant, y_0 has an actual physical interpretation. However, similarly the ω parameter in Fu's equation, κ is potentially an integrator of all other catchment properties than the aridity index.

3 Characteristics of the new framework

The obtained new formulation given in Eq. (9) is similar to Eq. (1), but includes y_0 as a new parameter (assuming $\kappa = 2.6$, corresponding to the original Budyko curve with

Title Page

Abstract

Introduction

Conclusions

References

Tables

Figures

◀

▶

◀

▶

Back

Close

Full Screen / Esc

Printer-friendly Version

Interactive Discussion



$\omega = 2.6$ and an example set of y_0 values, Fig. 2 shows a set of curves providing insights on the basic characteristics of the new equation).

First, if $y_0 = 0$ (being the original boundary condition) the obtained curve corresponds to the steady-state framework of Fu (1981) and Zhang et al. (2004), which is also evident from Eq. (9) and shows that both model formulations are consistently transferable. If $y_0 > 0$, the supply limit is systematically exceeded. The exceedance of the supply limit increases with increasing y_0 . If further $y_0 = 1$, the demand limit is reached. All curves are continuous and strictly increasing.

Taking a closer look at the underlying boundary conditions and definitions (see Sect. 2.1) reveals that y_0 implicitly accounts for the amount of additional water (besides water supplied through P) available for E . Since y_{\min} is explicitly defined to be the minimum of $y = (P - E)/E_p$, the quantity $y_0 = -y_{\min}$ physically represents the maximum fraction of E relative to E_p , which is not originating from P . A larger fraction consequently results in higher y_0 -values and thus in a stronger exceedance of the original supply limit. Further details on y_0 is provided in Sect. 4.

The sensitivity $\partial F(\Phi, \kappa, y_0)/\partial \Phi$ under varying κ and for three preselected values of y_0 is illustrated in Fig. 3. The sensitivity $\partial F(\Phi, \kappa, y_0)/\partial \Phi$ for different values of y_0 and κ shows the effect of the parameter choice on changes in E/P relative to changes in Φ . In general, the sensitivity is largest for small Φ (humid conditions), due to the fact that changes in E/P basically follow the demand limit (resulting in a sensitivity close to 1) regardless of parameter set (κ, y_0) . For different parameter settings, the sensitivity generally decreases with increasing Φ . For small values of y_0 (close to zero), sensitivity becomes smallest with increasing Φ , since small y_0 indicates conditions similar to steady-state conditions being constraint by the (horizontal and thus implying zero sensitivity) original supply limit. Further, the smallest sensitivity is reached for large values of κ . Large values of y_0 (close to 1) indicate conditions mainly constrained by the demand limit, thus implying a sensitivity close to 1.

A similar analysis is performed for varying values of κ under three preselected levels of y_0 (see Fig. 4). For $y_0 = 0$ (steady-state conditions), the sensitivity $\partial F/\partial \Phi$ is under

Title Page

Abstract

Introduction

Conclusions

References

Tables

Figures

◀

▶

◀

▶

Back

Close

Full Screen / Esc

Printer-friendly Version

Interactive Discussion



humid conditions ($\Phi < 1$) rather large, since changes in E/P are mainly constrained by demand limit. This especially applies for large values of κ . Under more arid conditions ($\Phi > 1$), the Budyko curve slowly converges towards the (horizontal) supply limit, resulting in a near-zero sensitivity. For $y_0 = 0.2$, denoting conditions relatively similar to steady-state conditions, the decrease in sensitivity with increasing Φ is weaker, whereas for $y_0 = 0.8$, denoting conditions where E is mainly constraint by the demand limit, sensitivity is large for large κ -values and decreases rather slowly with increasing Φ .

4 Interpreting the new parameter y_0

The new parameter y_0 is, in contrast to κ , physically well defined. The combination of Eqs. (4b) and (7) shows that y_0 is implicitly related to the amount of additional water (besides water supplied through P), which is available for E . If we rewrite Eq. (4b) with respect to y_0

$$y_0 = -y_{\min} = -\left(\frac{P-E}{E_p}\right)_{\min} = -\frac{P_{\min} - E_{\max}}{E_p}, \quad \text{if } P_{\min} - E_{\max} < 0, \quad (10)$$

where P_{\min} and E_{\max} are chosen in order to minimize y_{\min} for a given E_p , we obtain a linear equation in terms of aridity index

$$\left(\frac{E}{P}\right)_{\max} = y_0 \left(\frac{E_p}{P_{\min}}\right) + 1, \quad (11)$$

which constitutes the mathematical and physical meaning of y_0 within the new framework. That is, that y_0 determines the maximum slope of the upper limit, against which the obtained curve from Eq. (9) asymptotically converges to if $\kappa \rightarrow \infty$ (see Fig. 5). Physically, y_0 determines the maximum E/P that is reached in relation to Φ



within a certain time period and spatial domain. Technically speaking, y_0 determines the slope of the upper limit such that all possible pairs $(\Phi, E/P)$ are just below the line $y_0\Phi + 1$. It is further important to note that for mean annual conditions ($P - E \geq 0$), $y_0 = 0$ is considered, which results in a zero slope and thus determines the original supply limit of Eq. (1).

However, the actual slope m of the upper limit is smaller than y_0 , but directly related to both y_0 and κ as follows (see Appendix B for more information)

$$m = 1 - (1 - y_0)^{1 - \frac{1}{\kappa}}. \quad (12)$$

The relative difference between the maximum slope y_0 and the actual slope m of the upper limit (being the ratio of y_0/m) is thus determined following the relationship

$$\frac{y_0}{m} = (1 - y_0)^{1/\kappa}. \quad (13)$$

The ratio y_0/m as a function of both y_0 and κ is illustrated in Fig. 6. For small κ and large y_0 (close to 1), the difference between the actual slope m and the maximum slope y_0 is large, whereas for large κ the actual slope m converges towards y_0 . However, in any case, y_0 determines the maximum overshoot allowed with respect to the original supply limit at $y_0 = 0$.

Taking into account that y_0 is well-defined by Eq. (10), the parameter is in the following estimated from data. In the following, we use standard datasets of P , E and E_p to evaluate the performance of the obtained model described by Eq. (8).

5 Assessing the framework with observations

The new framework allows to compute E as a function of both P and E_p . Here we use well-established estimates of all three variables: Global Precipitation Climatology Project (GPCP) precipitation estimates, an E_p dataset (Sheffield et al., 2006, 2012)

Title Page

Abstract

Introduction

Conclusions

References

Tables

Figures

⏪

⏩

◀

▶

Back

Close

Full Screen / Esc

Printer-friendly Version

Interactive Discussion



based on the Penman–Monteith method (Monteith, 1965), and the LandFlux-Eval E estimates (Mueller et al., 2013), for the 1990–2000 time period and bilinearly interpolated to a unified 1° -grid.

We estimate the parameters κ and y_0 at gridpoint scale by determining y_0 from data (using Eq. 10) in order to obtain a fixed parameter for the whole time period. After y_0 is estimated, κ is estimated using a least squares fitting approach. However, estimating y_0 from data requires to find the set of (P, E, E_p) that minimizes Eq. (10) and results in the maximum slope of the adjusted supply limit. In order to account for the underlying data uncertainty and potential outliers, bootstrapping is used. The data cloud of a particular gridpoint is resampled 1000 times and for each sample the set of (P, E, E_p) that maximizes y_0 is selected. The median of all acquired y_0 -values is further used to estimate κ in a least squares fit.

The estimates of (κ, y_0) provide a fixed set of parameters that represents the whole time period and are illustrated in Fig. 7. The κ parameter is rather small in most subtropical desert regions and somewhat larger in tropical regions. Relatively large values of κ are further found in mid to high latitude regions. For y_0 , lowest values are found in tropical and midlatitude regions, whereas subtropical and also subpolar areas show somewhat higher values. In summary, dry regions tend to show values of y_0 close to zero, denoting conditions similar to the original framework. It is further important to note that κ and y_0 are spatially not correlated.

To validate the performance of the model given by Eq. (10), the derived set of parameters at each gridpoint is used to model E within the calibration period (1990–2000). Correlations between the modeled time series derived by using the parameter set and the observed time series and anomaly correlations between “detrended” time series with removed annual cycles are shown in Fig. 8.

Generally, correlations are relatively large in many regions, whereas anomaly correlations are smaller. Largest correlations (> 0.8) are found in all mid to high latitude regions. However, the most important feature regarding the time series of E in these regions is the annual cycle, which is well represented by the model. Hence, the first-

HESSD

12, 6799–6830, 2015

Nonstationary Budyko framework

P. Greve et al.

Title Page

Abstract

Introduction

Conclusions

References

Tables

Figures

◀

▶

◀

▶

Back

Close

Full Screen / Esc

Printer-friendly Version

Interactive Discussion



Nonstationary Budyko framework

P. Greve et al.

Title Page

Abstract

Introduction

Conclusions

References

Tables

Figures

◀

▶

◀

▶

Back

Close

Full Screen / Esc

Printer-friendly Version

Interactive Discussion



order control on E regarding seasonal variations is robustly represented by variations in water supply P and demand E_p . Further, correlations are, despite being still positive and relatively large (around 0.5), smaller in the inner tropics (central Amazonia and Congo Basin). This is most probably due to weak seasonal variations of E and hence an increased importance of second-order controls on month-to-month changes in E .

Similar to the original Budyko framework, this is however not true for deviations from the mean, which are potentially subject to various second-order controls, as suggested by very small anomaly correlations in most regions. However, in some subtropical areas, anomaly correlations are reasonably large (up to 0.5).

An interesting feature is found regarding many monsoon regions (India, Southeast Asia, Northeast Brazil and the Sahel). The distinct difference between wet and dry seasons seems to prohibit the use of a fixed parameter set. The derived parameter set instead represents wet season characteristics as y_0 and consequently overestimates dry season E . These issues could be circumvented by calibrating separate parameter sets for either each month of the year, or dry and wet seasons in particular. Using estimates of y_0 derived from monthly climatologies and corresponding κ -values represents seasonal variations in the parameters themselves. By doing so, resulting correlations in monsoon regions are similar to those in mid and high latitude regions (see Fig. 8c). Interestingly, using the individual parameter sets derived from monthly climatologies instead of using a fixed parameter set for the whole time period, does not significantly increase the performance of the model in mid to high latitude areas. It does further not significantly increase the capability of the model to predict anomalies (comparing Fig. 8b and d).

To further highlight the differences between midlatitude and monsoon regions, the model performance is analysed in more detail for two regions: (i) central Europe and (ii) central Sahel (see Fig. 9, regions are highlighted in Fig. 8). The upper two plots of Fig. 9 illustrate the respective data cloud of monthly values for both regions within the Budyko space. To note first, it is evident, that the original supply limit does not hold at monthly time scales as it is systematically overshoot. The data cloud for central

Europe shows an almost linear increase of E/P with increasing Φ , that is just slightly upset from the demand limit (thus implying a rather large y_0). For the central Sahel region, two regimes are noticeable. The first (during the winter months) being relatively similar to those of central Europe, with increasing E/P close to the demand limit (large y_0) and therefore depicting wet season conditions. The second regime (during spring and summer months) remains within the bounds of the original Budyko framework, hence depicting conditions of no additional water other than P available for E (therefore implying y_0 being close to zero).

The comparison between modeled and observed E reveals a rather good performance of the model for Central Europe ($R^2 = 0.87$, $RMSE = 0.51$). In the Sahel region, the fixed parameter set (see Fig. 9d) best represents the wet regime (as it determines the maximum slope), resulting in the model to overestimate dry season E . However, the model performs significantly better in the Sahel region if one explicitly accounts for seasonal variations in the parameter set (see Fig. 9f). For central Europe, however, it is evident that a monthly Climatology of parameter sets does not significantly improve the model performance.

It is further important to note, that in some instances also the demand limit is exceeded, occurring most probably due to data uncertainties regarding the E estimates and the E_p parametrization.

6 Conclusions

Our study introduces a new, two-parameter Budyko-like model, which is capable to represent non-stationary characteristics of E/P and E . The original Budyko framework is constrained to mean annual catchment scales, in order to ensure a steady-state water balance. Here we assume, that on most other spatio-temporal scales, the boundary condition constituted by the atmospheric water demand remains, whereas the boundary condition constituted by water supply is, besides P , also subject to water added (or withdrawn) via storage changes. To account for this assumption, the

Title Page

Abstract

Introduction

Conclusions

References

Tables

Figures

⏪

⏩

◀

▶

Back

Close

Full Screen / Esc

Printer-friendly Version

Interactive Discussion



Nonstationary
Budyko framework

P. Greve et al.

Title Page

Abstract

Introduction

Conclusions

References

Tables

Figures

I◀

▶I

◀

▶

Back

Close

Full Screen / Esc

Printer-friendly Version

Interactive Discussion



derivation of Fu's equation (Fu, 1981; Zhang et al., 2004) was modified accordingly and a similar formulation including an additional parameter is obtained. Although the parameter in the original and the first parameter of our formulation are purely mathematical, the additional parameter is physically well defined. Technically, the parameter rotates the original supply limit upwards. The framework was validated by using global, monthly, gridded standard estimates of P , E and E_p . The prediction of E using the model did represent seasonal dynamics for many parts of the world well by using a fixed parameter set over the whole time period. However, in several monsoon regions, the distinct difference between wet and dry seasons required enhanced parameter sets to represent the particular hydrological conditions of each month/season.

Like the original Budyko framework, the derived two-parameter Budyko model represents the influence of first-order controls (namely P and E_p , or in combination aridity index on water availability). Also, the combined influence of second-order controls (like e.g. vegetation, topography, etc.) are, comparable to Fu's equation, integrated into the first parameter of the framework (κ in the new framework, ω in Fu's equation, respectively). Studying these controls in Fu's formula was subject to numerous studies, but no conclusive assessment was conducted until present. Assessing the combined influence of climatic and catchment controls is hence clearly beyond the scope of this study. However, the additional second parameter of the new formulation y_0 is physically well defined as it represents a measure of additional water being (besides P) available for E . But the availability of additional water is itself subject to numerous controls and if no data is available, a direct estimation of the parameter is initially not possible. Assessing these controls is, however, subject to future research.

Finally we note that the available water that can compensate for lack of P , i.e. soil moisture, ground water and other surface water sources can be more accurately assessed on a month-to-month basis when using a water balance model. The purpose of the present formulation is not to replace such modeling approaches but to promote

a general framework accounting for non-stationary conditions within the Budyko relationship.

Further, Greve et al. (2015) recently suggested a probabilistic Budyko framework by assuming that the free parameter in Fu's equation is distributed. Similar assumptions could be applied to the two-parameter Budyko curve in future assessments, to allow for a better statistical representation of the scatter around the obtained curve.

Appendix A: Complete solution

Equations (3), (5) and (7) form a system of differential equations. A necessary condition to solve this system is

$$\frac{\partial f(x)}{\partial E_p} + \frac{\partial f(x)}{\partial E} g(y) = \frac{\partial g(y)}{\partial P} + \frac{\partial g(y)}{\partial E} f(x) \quad (\text{A1})$$

Combining Eq. (A1) with Eq. (4) yields

$$\frac{\partial f(x)}{\partial E_p} = \frac{\partial f(x)}{\partial E_p} \frac{\partial x}{\partial x} = \frac{1}{P} \left(1 - \frac{\partial E}{\partial E_p} \right) \frac{\partial f(x)}{\partial x} = \frac{1}{P} (1 - g(y)) \frac{\partial f(x)}{\partial x} \quad (\text{A2a})$$

$$\frac{\partial f(x)}{\partial E} = \frac{\partial f(x)}{\partial E} \frac{\partial x}{\partial x} = \frac{1}{P} \left(\frac{\partial E_p}{\partial E} - 1 \right) \frac{\partial f(x)}{\partial x} = \frac{1}{P} \left(\frac{1}{g(y)} - 1 \right) \frac{\partial f(x)}{\partial x} \quad (\text{A2b})$$

$$\frac{\partial g(y)}{\partial P} = \frac{\partial g(y)}{\partial P} \frac{\partial y}{\partial y} = \frac{1}{E_p} \left(1 - \frac{\partial E}{\partial P} \right) \frac{\partial g(y)}{\partial y} = \frac{1}{E_p} (1 - f(x)) \frac{\partial g(y)}{\partial y} \quad (\text{A2c})$$

$$\frac{\partial g(y)}{\partial E} = \frac{\partial g(y)}{\partial E} \frac{\partial y}{\partial y} = \frac{1}{E_p} \left(\frac{\partial P}{\partial E} - 1 \right) \frac{\partial g(y)}{\partial y} = \frac{1}{E_p} \left(\frac{1}{f(x)} - 1 \right) \frac{\partial g(y)}{\partial y} \quad (\text{A2d})$$

Substituting the factors in Eq. (A1) with those given in Eq. (A2) gives:

$$\frac{\partial f(x)}{\partial x} \left((1 - g(y)) + \left(\frac{1}{g(y)} - 1 \right) g(y) \right) = \frac{P}{E_p} \frac{\partial g(y)}{\partial y} \left((1 - f(x)) + \left(\frac{1}{f(x)} - 1 \right) f(x) \right)$$

$$(1 - g(y)) \frac{\partial f(x)}{\partial x} = \frac{P}{E_p} (1 - f(x)) \frac{\partial g(y)}{\partial y} \quad (\text{A3})$$

Expanding P/E_p yields under consideration of Eq. (4)

$$\frac{P}{E_p} = \frac{\frac{E_p + P - E}{E_p}}{\frac{E_p + P - E}{P}} = \frac{1 + \frac{P - E}{E_p}}{1 + \frac{E_p - E}{P}} = \frac{1 + y}{1 + x} \quad (\text{A4})$$

From Eq. (A3) and Eq. (A4) follows

$$(1 - g(y)) \frac{\partial f(x)}{\partial x} = \frac{1 + y}{1 + x} (1 - f(x)) \frac{\partial g(y)}{\partial y}$$

$$\frac{1 + x}{1 - f(x)} \frac{\partial f(x)}{\partial x} = \frac{1 + y}{1 - g(y)} \frac{\partial g(y)}{\partial y} \quad (\text{A5})$$

where each side is a function of x or y only. Assuming the result of each side is α it follows

$$\frac{1 + x}{1 - f(x)} \frac{\partial f(x)}{\partial x} = \alpha \quad (\text{A6a})$$

$$\frac{1 + y}{1 - g(y)} \frac{\partial g(y)}{\partial y} = \alpha \quad (\text{A6b})$$

Title Page

Abstract

Introduction

Conclusions

References

Tables

Figures

◀

▶

◀

▶

Back

Close

Full Screen / Esc

Printer-friendly Version

Interactive Discussion



Integrating Eq. (A6a) under consideration of the boundary condition given by Eq. (5) leads to the following expression for $f(x)$

$$\int_0^x \frac{1}{1-f(t)} \frac{\partial f(t)}{\partial t} dt = \alpha \int_0^x \frac{1}{1-t} dt$$

$$[-\ln(1-f(t))]_0^x = \alpha [\ln(1+t)]_0^x$$

$$\ln(1-f(x)) = -\alpha \ln(1+x)$$

$$1-f(x) = (1+x)^{-\alpha}$$

$$f(x) = 1 - (1+x)^{-\alpha} \tag{A7}$$

Integrating Eq. (A6b) is different from the traditional solution given in Zhang et al. (2004), as we are using the new boundary condition given by Eq. (7)

$$\int_{-y_0}^y \frac{1}{1-g(t)} \frac{\partial g(t)}{\partial t} dt = \alpha \int_{-y_0}^y \frac{1}{1-t} dt$$

$$[-\ln(1-g(t))]_{-y_0}^y = \alpha [\ln(1+t)]_{-y_0}^y$$

$$\ln(1-g(y)) - \ln(1-g(-y_0)) = \alpha (\ln(1-y_0) - \ln(1+y))$$

$$\ln(1-g(y)) = \alpha \ln \left(\frac{1-y_0}{1+y} \right)$$

$$1-g(y) = \left(\frac{1-y_0}{1+y} \right)^\alpha$$

$$g(y) = 1 - \left(\frac{1-y_0}{1+y} \right)^\alpha \tag{A8}$$

Title Page

Abstract

Introduction

Conclusions

References

Tables

Figures

⏪

⏩

◀

▶

Back

Close

Full Screen / Esc

Printer-friendly Version

Interactive Discussion



Considering the expansion from Eq. (A4) finally gives

$$\partial E / \partial P = 1 - (1 + x)^{-\alpha} = 1 - \left(\frac{P}{E_p + P - E} \right)^\alpha \quad (\text{A9})$$

$$\partial E / \partial E_0 = 1 - (1 - y_0)^\alpha (1 + y)^{-\alpha} = 1 - (1 - y_0)^\alpha \left(\frac{E_0}{E_0 + P - E} \right)^\alpha \quad (\text{A10})$$

In the next step, Eq. (A9) is integrated over P . As Eq. (A9) is identical to those in Zhang et al. (2004), we follow their substitution approach. It follows

$$E = E_0 + P - (k + P^{\alpha+1})^{\frac{1}{\alpha+1}} \quad (\text{A11})$$

where k is a function of E_0 only. Differentiate Eq. (A11) with respect to E_0 gives an estimate of $\partial E / \partial E_0$, which used with Eq. (A10) determines k

$$\frac{\partial E}{\partial E_0} = 1 - \frac{1}{\alpha + 1} (k + P^{\alpha+1})^{-\frac{\alpha}{\alpha+1}} \frac{\partial k}{\partial E_0} = 1 - (1 - y_0)^\alpha \left(\frac{E_0}{E_0 + P - E} \right)^\alpha \quad (\text{A12})$$

This leads under consideration of Eq. (A11) to the following expression

$$\begin{aligned} \frac{\partial k}{\partial E_0} &= (\alpha + 1)(1 - y_0)^\alpha \left(\frac{E_0}{E_0 + P - E} \right)^\alpha (k + P^{\alpha+1})^{\frac{\alpha}{\alpha+1}} \\ &= (\alpha + 1)(1 - y_0)^\alpha \left(\frac{E_0}{E_0 + P - (E_0 + P - (k + P^{\alpha+1})^{\frac{1}{\alpha+1}})} \right)^\alpha (k + P^{\alpha+1})^{\frac{\alpha}{\alpha+1}} \\ &= (\alpha + 1)(1 - y_0)^\alpha E_0^\alpha \\ k &= (\alpha + 1)(1 - y_0)^\alpha \int E_0^\alpha dE_0 \\ k &= (1 - y_0)^\alpha E_0^{\alpha+1} + C \end{aligned} \quad (\text{A13})$$

with C being an integration constant. Substituting Eq. (A13) back into Eq. (A11), one obtains the following expression

$$E = E_0 + P - \left((1 - y_0)^\alpha E_0^{\alpha+1} + C + P^{\alpha+1} \right)^{\frac{1}{\alpha+1}} \quad (\text{A14})$$

and as $\lim_{P \rightarrow 0} E = 0$ follows $C = 0$. Substituting $\kappa = \alpha + 1$ finally gives

$$E = E_p + P - \left((1 - y_0)^{\kappa-1} E_p^\kappa + P^\kappa \right)^{\frac{1}{\kappa}} \quad (\text{A15})$$

and further provides by writing $\Phi = E_p/P$

$$\frac{E}{P} = 1 + \Phi - \left(1 + (1 - y_0)^{\kappa-1} (\Phi)^\kappa \right)^{\frac{1}{\kappa}} \quad (\text{A16})$$

$$F \left(\frac{E}{E_p}, \kappa, y_0 \right) = \frac{E}{E_p} = 1 + \frac{P}{E_p} - \left((1 - y_0)^{\kappa-1} + \left(\frac{P}{E_p} \right)^\kappa \right)^{\frac{1}{\kappa}} \quad (\text{A17})$$

HESSD

12, 6799–6830, 2015

Nonstationary Budyko framework

P. Greve et al.

Title Page

Abstract

Introduction

Conclusions

References

Tables

Figures

◀

▶

◀

▶

Back

Close

Full Screen / Esc

Printer-friendly Version

Interactive Discussion



Appendix B: Solution of the actual slope

The actual slope m of the upper limit against which the obtained Budyko curve is converging to is smaller than y_0 . We introduced Eq. (12) to calculate m and in the following we provide the complete solution in order to obtain Eq. (12).

5 The value of m is the slope of the linear function $m\Phi + 1$ that forms the asymptote to $F(\Phi, \kappa, y_0)$ given by Eq. (9). Hence,

$$\lim_{\Phi \rightarrow \infty} [F(\Phi, \kappa, y_0) - (m\Phi + 1)] = 0. \quad (\text{B1})$$

Using Eq. (9) and dividing by Φ yields

$$\lim_{\Phi \rightarrow \infty} \left[\frac{\left(1 + (1 - y_0)^{\kappa-1} (\Phi)^\kappa\right)^{\frac{1}{\kappa}}}{\Phi} + 1 - m \right] = 0. \quad (\text{B2})$$

10 By raising the term in brackets to the power of κ one obtains

$$\lim_{\Phi \rightarrow \infty} \left[(1 - m)^\kappa - \Phi^{-\kappa} \left(1 + \Phi^\kappa (1 - y_0)^{\kappa-1}\right) \right] = 0, \quad (\text{B3})$$

and it follows

$$\lim_{\Phi \rightarrow \infty} \left[(1 - m)^\kappa - (1 - y_0)^{\kappa-1} - \Phi^{-\kappa} \right] = 0. \quad (\text{B4})$$

Since $\Phi^{-\kappa} \rightarrow 0$ for $\Phi \rightarrow \infty$ we obtain

$$15 (1 - m)^\kappa = (1 - y_0)^{\kappa-1}. \quad (\text{B5})$$

Solving for m yields

$$m = (1 - y_0)^{1 - \frac{1}{\kappa}}. \quad (\text{B6})$$

Acknowledgements. The Center for Climate Systems Modeling (C2SM) at ETH Zurich is acknowledged for providing technical and scientific support. We acknowledge partial support from the ETH Research Grant CH2-01 11-1, EU-FP7 EMBRACE and the ERC DROUGHT-HEAT Project.

5 References

- Berghuijs, W. R., Woods, R. A., and Hrachowitz, M.: A precipitation shift from snow towards rain leads to a decrease in streamflow, *Nature Climate Change*, 4, 583–586, 2014. 6801
- Budyko, M.: *Climate and Life*, Academic Press, New York, USA, 1974. 6800
- Budyko, M. I.: *The Heat Balance of the Earth's Surface*, Gidrometeoizdat, Leningrad, 1956 (in Russian). 6800
- Chen, X., Alimohammadi, N., and Wang, D.: Modeling interannual variability of seasonal evaporation and storage change based on the extended Budyko framework, *Water Resour. Res.*, 49, 6067–6078, 2013. 6801, 6802
- Choudhury, B.: Evaluation of an empirical equation for annual evaporation using field observations and results from a biophysical model, *J. Hydrol.*, 216, 99–110, 1999. 6800
- Donohue, R. J., Roderick, M. L., and McVicar, T. R.: On the importance of including vegetation dynamics in Budyko's hydrological model, *Hydrol. Earth Syst. Sci.*, 11, 983–995, doi:10.5194/hess-11-983-2007, 2007. 6801
- Donohue, R. J., Roderick, M. L., and McVicar, T. R.: Roots, storms and soil pores: incorporating key ecohydrological processes into Budyko's hydrological model, *J. Hydrol.*, 436–437, 35–50, 2012. 6801
- Fu, B.: On the calculation of the evaporation from land surface, *Scientia Atmospherica Sinica*, 1, 23–31, 1981 (in Chinese). 6800, 6801, 6802, 6803, 6805, 6811
- Gentine, P., D'Odorico, P., Lintner, B. R., Sivandran, G., and Salvucci, G.: Interdependence of climate, soil, and vegetation as constrained by the Budyko curve, *Geophys. Res. Lett.*, 39, L19404, doi:10.1029/2012GL053492, 2012. 6801
- Greve, P., Gudmundsson, L., Orłowsky, B., and Seneviratne, S.: Introducing a probabilistic Budyko framework, *Geophys. Res. Lett.*, 42, 2261–2269, doi:10.1002/2015GL063449, 2015. 6812

Nonstationary Budyko framework

P. Greve et al.

Title Page

Abstract

Introduction

Conclusions

References

Tables

Figures

⏪

⏩

◀

▶

Back

Close

Full Screen / Esc

Printer-friendly Version

Interactive Discussion



Nonstationary
Budyko framework

P. Greve et al.

[Title Page](#)[Abstract](#)[Introduction](#)[Conclusions](#)[References](#)[Tables](#)[Figures](#)[⏪](#)[⏩](#)[◀](#)[▶](#)[Back](#)[Close](#)[Full Screen / Esc](#)[Printer-friendly Version](#)[Interactive Discussion](#)

- Li, D., Pan, M., Cong, Z., Zhang, L., and Wood, E.: Vegetation control on water and energy balance within the Budyko framework, *Water Resour. Res.*, 49, 969–976, 2013. 6801
- Mezentsev, V.: More on the computation of total evaporation (Yechio raz o rastchetie srednevo summarnovo ispareniiia), *Meteorog. i Gridrolog.*, 5, 24–26, 1955. 6800
- 5 Milly, P. C. D.: An analytic solution of the stochastic storage problem applicable to soil water, *Water Resour. Res.*, 29, 3755–3758, 1993. 6802
- Milly, P. C. D.: Climate, soil water storage, and the average annual water balance, *Water Resour. Res.*, 30, 2143–2156, 1994. 6801
- Monteith, J.: Evaporation and environment, *Sym. Soc. Exp. Biol.*, 19, 205–234, 1965. 6808
- 10 Mueller, B., Hirschi, M., Jimenez, C., Ciais, P., Dirmeyer, P. A., Dolman, A. J., Fisher, J. B., Jung, M., Ludwig, F., Maignan, F., Miralles, D. G., McCabe, M. F., Reichstein, M., Sheffield, J., Wang, K., Wood, E. F., Zhang, Y., and Seneviratne, S. I.: Benchmark products for land evapotranspiration: LandFlux-EVAL multi-data set synthesis, *Hydrol. Earth Syst. Sci.*, 17, 3707–3720, doi:10.5194/hess-17-3707-2013, 2013. 6808
- 15 Ol'Dekop, E. M.: On Evaporation From the Surface of River Basins, Univ. of Tartu, Tartu, Estonia, 1911. 6800
- Orlowsky, B. and Seneviratne, S. I.: Elusive drought: uncertainty in observed trends and short- and long-term CMIP5 projections, *Hydrol. Earth Syst. Sci.*, 17, 1765–1781, doi:10.5194/hess-17-1765-2013, 2013. 6802
- 20 Pike, J. G.: The estimation of annual run-off from meteorological data in a tropical climate, *J. Hydrol.*, 2, 116–123, 1964. 6800
- Porporato, A., Daly, E., and Rodriguez-Iturbe, I.: Soil water balance and ecosystem response to climate change, *Am. Nat.*, 164, 625–632, 2004. 6800, 6801
- Potter, N. J. and Zhang, L.: Water balance variability at the interstorm timescale, *Water Resour. Res.*, 43, W05405, doi:10.1029/2006WR005276, 2007. 6802
- 25 Potter, N. J., Zhang, L., Milly, P. C. D., McMahon, T. A., and Jakeman, A. J.: Effects of rainfall seasonality and soil moisture capacity on mean annual water balance for Australian catchments, *Water Resour. Res.*, 41, W06007, doi:10.1029/2004WR003697, 2005. 6801
- Schreiber, P.: Ueber die Beziehungen zwischen dem Niederschlag und der Wasserfuehrung der Fluesse in Mitteleuropa, *Z. Meteorol.*, 21, 441–452, 1904. 6800
- 30 Shao, Q., Traylen, A., and Zhang, L.: Nonparametric method for estimating the effects of climatic and catchment characteristics on mean annual evapotranspiration, *Water Resour. Res.*, 48, W03517, doi:10.1029/2010WR009610 2012. 6801

Nonstationary Budyko framework

P. Greve et al.

Title Page

Abstract

Introduction

Conclusions

References

Tables

Figures

⏪

⏩

◀

▶

Back

Close

Full Screen / Esc

Printer-friendly Version

Interactive Discussion



Sheffield, J., Goteti, G., and Wood, E. F.: Development of a 50-year high-resolution global dataset of meteorological forcings for land surface modeling, *J. Climate*, 19, 3088–3111, 2006. 6807

Sheffield, J., Wood, E. F., and Roderick, M. L.: Little change in global drought over the past 60 years, *Nature*, 491, 435–438, 2012. 6807

Turc, L.-H.: Le Bilan d'eau des sols: relations entre les précipitations, l'évaporation et l'écoulement. . . Institut national de la recherche agronomique, Paris, 1955. 6800

Wang, D., and Tang, Y.: A One-parameter Budyko model for water balance captures emergent behavior in Darwinian hydrologic models, *Geophys. Res. Lett.*, 41, 4569–4577, doi:10.1002/2014GL060509 2014. 6801

Wang, G.: Agricultural drought in a future climate: results from 15 global climate models participating in the IPCC 4th assessment, *Clim. Dynam.*, 25, 739–753, 2005. 6802

Williams, C. A., Reichstein, M., Buchmann, N., Baldocchi, D., Beer, C., Schwalm, C., Wohlfahrt, G., Hasler, N., Bernhofer, C., Foken, T., Papale, D., Schymanski, S., and Schaefer, K.: Climate and vegetation controls on the surface water balance: synthesis of evapotranspiration measured across a global network of flux towers, *Water Resour. Res.*, 48, W06523, doi:10.1029/2011WR011586 2012. 6801

Xu, X., Liu, W., Scanlon, B. R., Zhang, L., and Pan, M.: Local and global factors controlling water-energy balances within the Budyko framework, *Geophys. Res. Lett.*, 40, 6123–6129, 2013. 6801

Yang, D., Sun, F., Liu, Z., Cong, Z., Ni, G., and Lei, Z.: Analyzing spatial and temporal variability of annual water-energy balance in nonhumid regions of China using the Budyko hypothesis, *Water Resour. Res.*, 43, W04426, doi:10.1029/2006WR005224, 2007. 6801

Yang, H., Yang, D., Lei, Z., and Sun, F.: New analytical derivation of the mean annual water-energy balance equation, *Water Resour. Res.*, 44, W03410, doi:10.1029/2007WR006135, 2008. 6800

Zhang, L., Dawes, W. R., and Walker, G. R.: Response of mean annual evapotranspiration to vegetation changes at catchment scale, *Water Resour. Res.*, 37, 701–708, 2001. 6800, 6801

Zhang, L., Hickel, K., Dawes, W. R., Chiew, F. H. S., Western, A. W., and Briggs, P. R.: A rational function approach for estimating mean annual evapotranspiration, *Water Resour. Res.*, 40, W02502, doi:10.1029/2003WR002710 2004 6800, 6801, 6802, 6805, 6811

Zhang, L., Potter, N., Hicel, K., Zhang, Y., and Shao, Q.: Water balance modeling over variable time scales based on the Budyko framework – model development and testing, *J. Hydrol.*, 360, 117–131, 2008. 6802

5 Zhou, G., Wei, X., Chen, X., Zhou, P., Liu, X., Xiao, Y., Sun, G., Scott, D. F., Zhou, S., Han, L., and Su, Y.: Global pattern for the effect of climate and land cover on water yield, *Nature Communications*, 6, 5918, doi:10.1038/ncomms6918, 2015a. 6801

Zhou, S., Yu, B., Huang, Y., and Wang, G.: The complementary relationship and generation of the Budyko functions, *Geophys. Res. Lett.*, 42, 1781–1790, doi:10.1002/2015GL063511, 2015b. 6801

HESSD

12, 6799–6830, 2015

Nonstationary Budyko framework

P. Greve et al.

[Title Page](#)

[Abstract](#)

[Introduction](#)

[Conclusions](#)

[References](#)

[Tables](#)

[Figures](#)



[Back](#)

[Close](#)

[Full Screen / Esc](#)

[Printer-friendly Version](#)

[Interactive Discussion](#)



HESD

12, 6799–6830, 2015

Nonstationary Budyko framework

P. Greve et al.

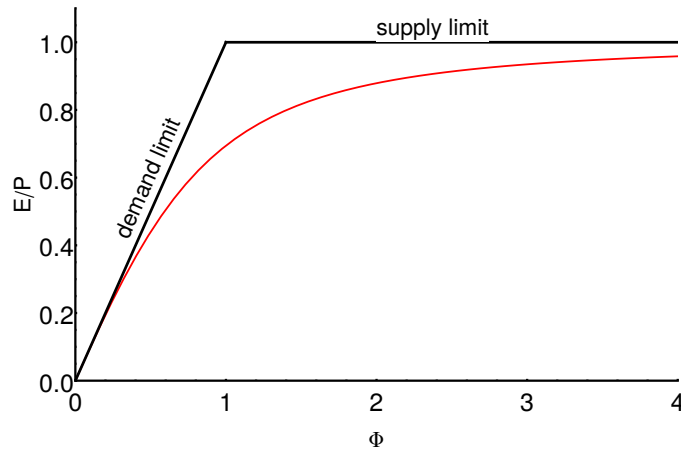


Figure 1. The original Budyko curve (red), limited by both the demand limit ($E = E_p$) and the supply limit ($E = P$).

Title Page

Abstract

Introduction

Conclusions

References

Tables

Figures

◀

▶

◀

▶

Back

Close

Full Screen / Esc

Printer-friendly Version

Interactive Discussion



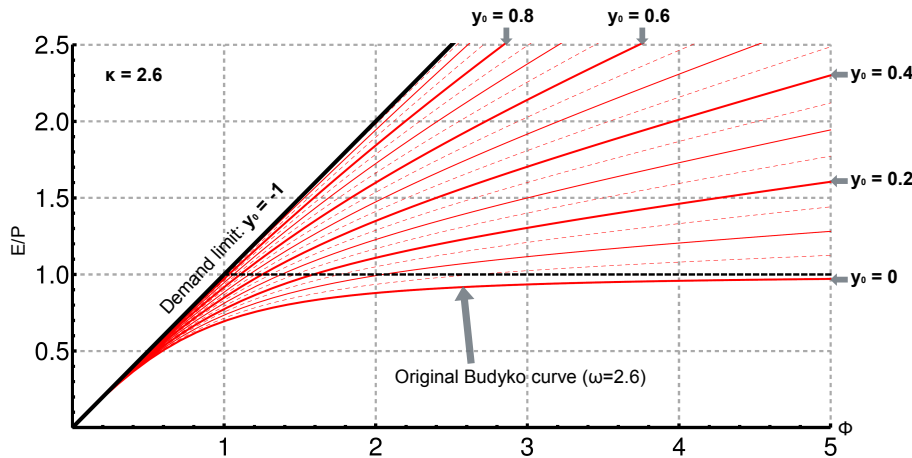


Figure 2. Set of curves of the new framework for $\kappa = 2.6$ and different y_0 . Note that the obtained curve for the parameter set $(\kappa, y_0) = (2.6, 0)$ corresponds to the original Budyko curve ($\omega = 2.6$). The supply limit (dashed black line) is systematically exceeded if $y_0 < 0$ and the demand limit (solid black line) is reached if $y_0 = -1$.

Title Page	
Abstract	Introduction
Conclusions	References
Tables	Figures
◀	▶
◀	▶
Back	Close
Full Screen / Esc	
Printer-friendly Version	
Interactive Discussion	



Nonstationary
Budyko framework

P. Greve et al.

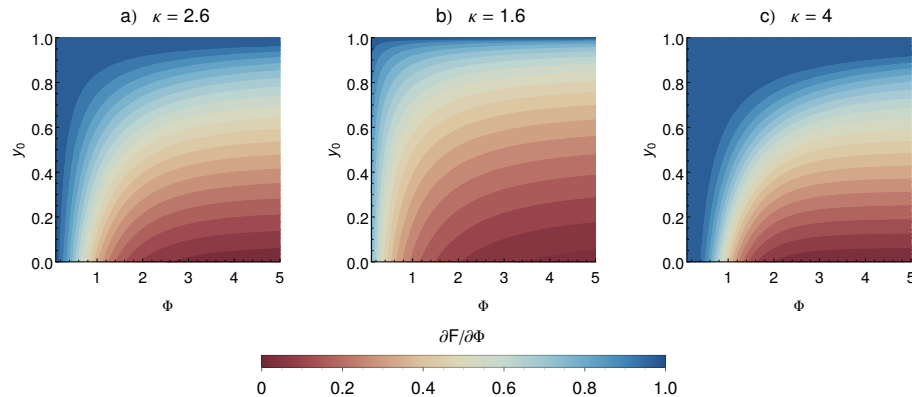


Figure 3. The sensitivity $\partial F / \partial \Phi$ under varying y_0 , for $\kappa = 2.6$ (left, similar to the original Budyko framework if $y_0 = 0$), $\kappa = 1.6$ (center) and $\kappa = 4$ (right). Blueish colors denote high, reddish colors low sensitivity.

[Title Page](#)[Abstract](#)[Introduction](#)[Conclusions](#)[References](#)[Tables](#)[Figures](#)[I ◀](#)[▶ I](#)[◀](#)[▶](#)[Back](#)[Close](#)[Full Screen / Esc](#)[Printer-friendly Version](#)[Interactive Discussion](#)

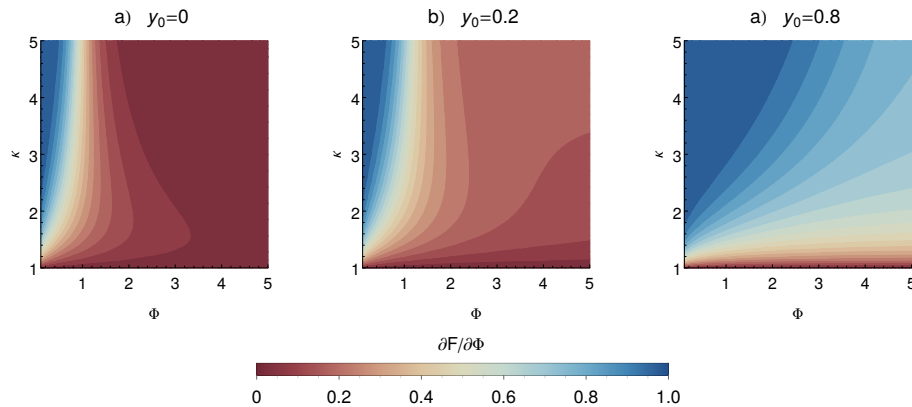


Figure 4. The sensitivity $\partial F/\partial \Phi$ under varying κ , for $y_0 = 0$ (left), $y_0 = -0.2$ (center) and $y_0 = -0.8$ (right). Blueish colors denote high, reddish colors low sensitivity.

[Title Page](#)[Abstract](#)[Introduction](#)[Conclusions](#)[References](#)[Tables](#)[Figures](#)[⏪](#)[⏩](#)[◀](#)[▶](#)[Back](#)[Close](#)[Full Screen / Esc](#)[Printer-friendly Version](#)[Interactive Discussion](#)

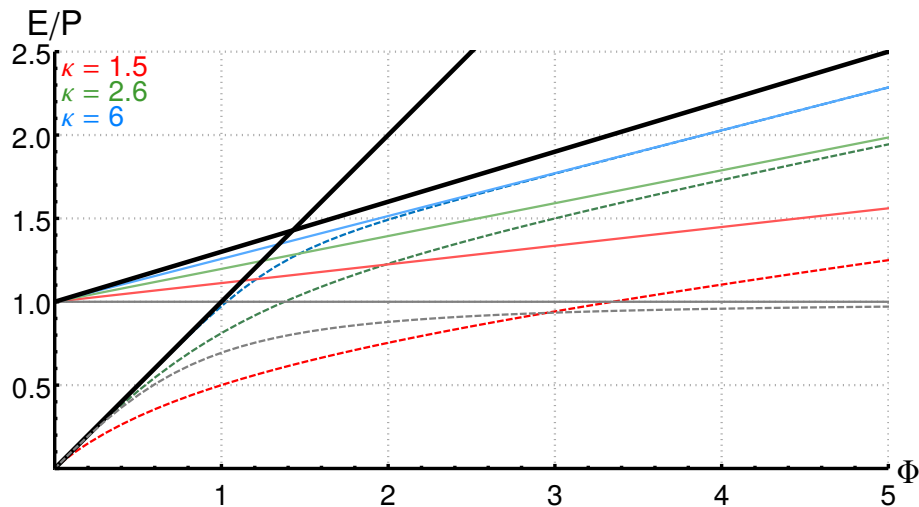


Figure 5. Difference between the actual (solid colored lines) and maximum slope (solid black line) of the supply limit for different values of κ (red: $\kappa = 1.5$, green: $\kappa = 2.6$ and blue: $\kappa = 6$) and $y_0 = -0.3$. The maximum slope ($m = y_0 = -0.3$) is reached if $\kappa \rightarrow \infty$.

[Title Page](#)
[Abstract](#)
[Introduction](#)
[Conclusions](#)
[References](#)
[Tables](#)
[Figures](#)
[I◀](#)
[▶I](#)
[◀](#)
[▶](#)
[Back](#)
[Close](#)
[Full Screen / Esc](#)
[Printer-friendly Version](#)
[Interactive Discussion](#)

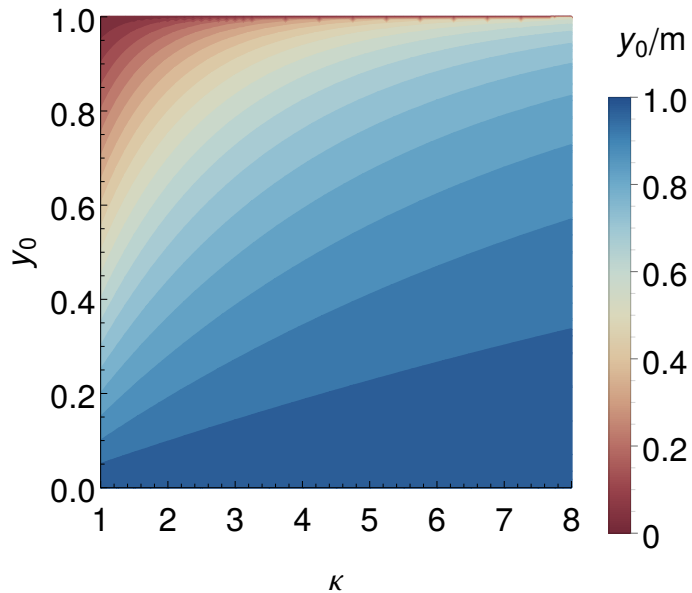



Figure 6. The ratio $-y_0/m$ as a function of both y_0 and κ estimated from Eq. (13).

Title Page

Abstract	Introduction
Conclusions	References
Tables	Figures

◀
▶

◀
▶

Back Close

Full Screen / Esc

Printer-friendly Version

Interactive Discussion



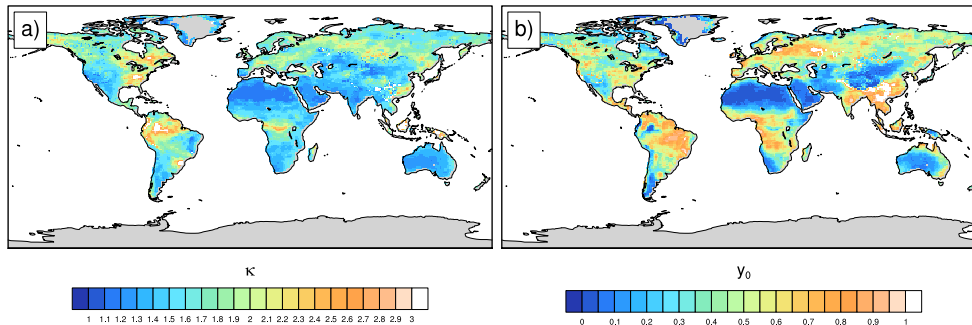


Figure 7. Estimated values of κ (subfigure **a**) estimated in a least squares fitting after values of y_0 (subfigure **b**) were directly estimated from all data at each grid point using standard monthly datasets of P , E and E_p within the 1990–2000 period.

[Title Page](#)[Abstract](#)[Introduction](#)[Conclusions](#)[References](#)[Tables](#)[Figures](#)[⏪](#)[⏩](#)[◀](#)[▶](#)[Back](#)[Close](#)[Full Screen / Esc](#)[Printer-friendly Version](#)[Interactive Discussion](#)

Nonstationary
Budyko framework

P. Greve et al.

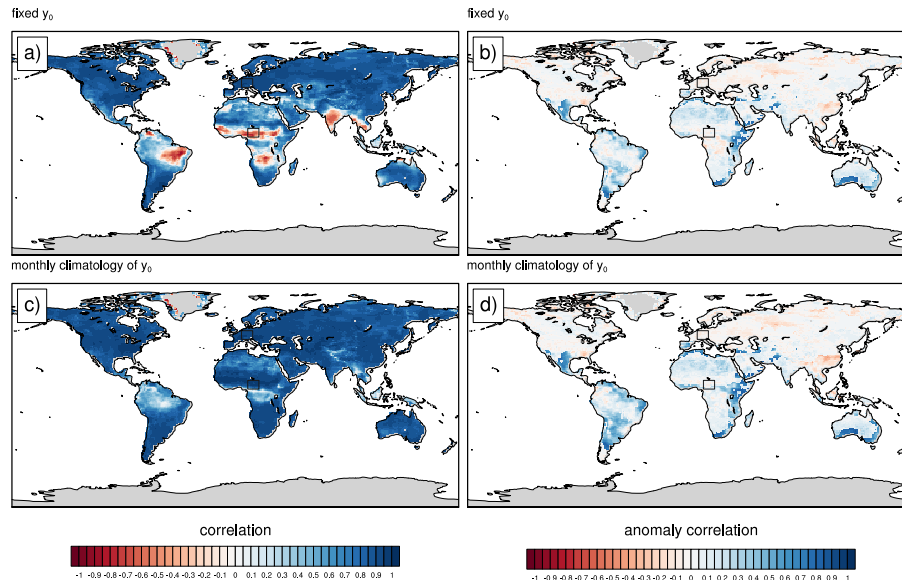


Figure 8. Correlation between modeled E and observed E for (a) the fixed estimated parameter set estimated for the whole time period and (c) parameter sets derived from monthly climatologies. Anomaly correlations of the detrended time series after removing the annual cycle of E are depicted in subfigure (b, d). Grey boxes indicate the regions featured in Fig. 9.

Title Page

Abstract

Introduction

Conclusions

References

Tables

Figures

◀

▶

◀

▶

Back

Close

Full Screen / Esc

Printer-friendly Version

Interactive Discussion



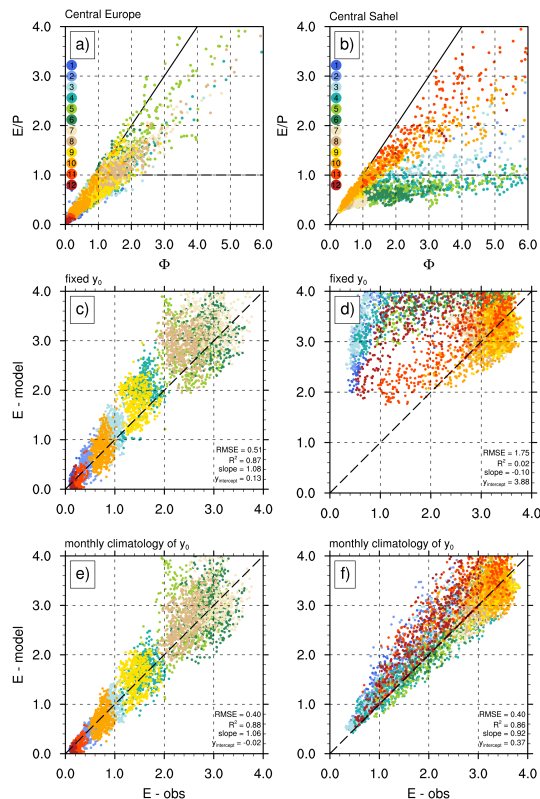


Figure 9. Data cloud of monthly values within the Budyko space for all gridboxes in (a) central Europe (45–53° N, 5–14° E) and (b) parts of the Sahel (5–12° N, 10–19° E, see also Fig. 8). The black solid line denotes the demand limit, the dashed line denotes the original supply limit. (c, d) Scatter plots of modeled vs. observed E using the fixed estimated parameter set and (e, f) using the parameter sets derived from monthly climatologies, at each gridbox within the particular regions (left column: central Europe, right: Sahel). Months of the year are color-coded.